ELSEVIER

Journal of Chromatography A, 780 (1997) 93–102

JOURNAL OF CHROMATOGRAPHY A

Review

Microemulsions in separation sciences

Hitoshi Watarai

Osaka University, Graduate School of Science, Department of Chemistry, Toyonaka, Osaka 560, Japan

Abstract

Fundamental properties of microemulsions in relation to their utilization in liquid state separation methods of ionic and non-ionic compounds are briefly reviewed. Discussions are focused on some characteristic functions of o/w (L_1) and w/o (L_2) single-phase microemulsions and the two-phase microemulsion systems of Winsor I and Winsor II from the viewpoint of their use as separation media in solvent extraction, liquid chromatography and capillary electrophoresis. Through reviewing, practical advantages of the microemulsion media in the separation of metal ions and biological compounds are assessed. © 1997 Elsevier Science B.V.

Keywords: Reviews; Microemulsions; Mobile phase composition; Microscopic partition

Contents

1. Introduction

Microemulsions, which are made from water, an organic solvent, and a surfactant and occasionally an alcohol as a cosurfactant, have unique properties as separation media such as the nanometer-sized spherical or bicontinuous structure, the rapid coalescence and reseparation dynamics of the structure and the enhanced solubilization capacity. Microemulsion can be used as a pseudo-single-phase solvent or two-phase solvent consisting of a microemulsion phase and an aqueous or organic phase. In the single phase w/o and o/w microemulsions, which are denoted as L_1 and L_2, respectively [1], the partition and the interfacial adsorption of a solute in the micro-heterogeneous systems are responsible for the chemical reactivity and separation mechanisms. The nanometer-sized structure brings about an extraordi-

0021-9673/97/$17.00 © 1997 Elsevier Science B.V. All rights reserved.
PII S0021-9673(97)00444-5

narily large specific interfacial area to the microemulsion systems. Thus, the interfacial adsorption at the micro-droplet surface becomes a significant factor determining the solubilization capacity. In two-phase systems, the distribution equilibria between the bulk phases and the mass-transfer through the interface are imposed on the single phase phenomena. In the extraction kinetics of metal ions or proteins, the structure and physicochemical properties of the interfacial monolayer can also play an important role.

The multiphase microemulsion-containing systems were first described by Winsor [2]. There are three possibilities for the type of phases depending on the compositions, temperature and salinity. Two-phase systems, called Winsor I and Winsor II, correspond to an o/w microemulsion coexisting with an oil phase and a w/o microemulsion coexisting with excess water, respectively. A Winsor III system forms when the surfactant is concentrated in a middle phase, which coexists with oil and water. The Winsor III and Winsor II systems have been employed as solvent extraction media of metal ions and biological substances.

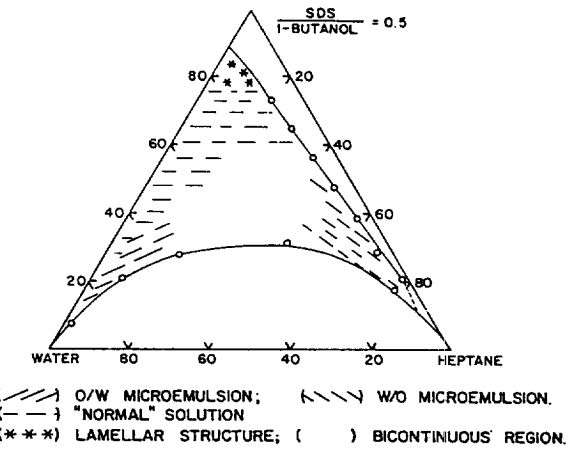

Fig. 1. Schematic representation of ternary diagram of the system SDS–1-butanol–water–heptane at surfactant–alcohol ratio of 0.5 (weight fraction) [3].

2. Formation of microemulsions

Isothermal phase diagram of three or four components can represent the region of a transparent, isotropic and low-viscous microemulsion phase along with those of a liquid crystalline phase or a lamellar phase. In general, o/w microemulsion is prepared in the water-rich region and w/o microemulsion in the organic-rich region. For example, the ternary diagram of the system SDS–1-butanol–water–heptane at surfactant–alcohol ratio of 0.5 shows the formation of o/w microemulsions near the corner of water as shown in Fig. 1 [3,4]. The increase in a salinity or temperature decreases the solubility of the organic component in water and enhances a phase separation, which results in the transition of Winsor I→Winsor III→Winsor II as illustrated in Fig. 2 [5–7]. As for the surfactants, ionic metal extractants can also form microemulsions as well as common ionic and non-ionic surfactants, e.g., quaternary alkylammonium salts, alkylsulphate and polyoxyethyl ether. Bis(2-ethylhexyl) hydrogenphosphate (HDEHP) and its sodium [8] or ammonium [9] salts, which are metal extractable anionic surfactants, bear a strong resemblance to sodium bis(2-ethylhexyl) sulfosuccinate (Aerosol OT

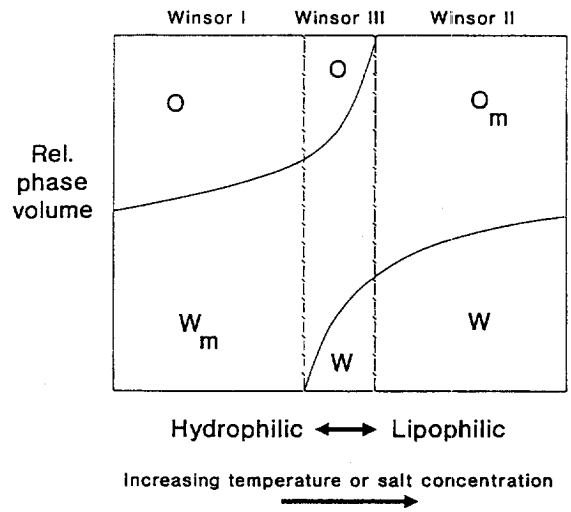

Fig. 2. Schematic illustration of changes in volume fractions of each phase in a mixture of water and oil containing a finite amount of surfactant: o=excess oil; o_m=w/o microemulsion; w=excess water; w_m=o/w microemulsion. The middle phase is a microemulsion [5].

or AOT) which is very efficient at stabilizing w/o microemulsions [10]. Recently, dioleyl phosphoric acid (DOLPA) was reported as the best surfactant currently available for protein extraction [11].

The geometry of the microemulsions is primarily dependent on the Israelachvili–Ninham packing parameter of the surfactant, $P=v_{eff}/a_h l_s$ where v_{eff}, a_h and l_s refer to the effective tail volume, the topological surface area of headgroup of monomer and the length of surfactant, respectively [12,13]; a normal spherical shape for $P<1$, a lamellar or bicontinuous shape for $P\fallingdotseq 1$, and a reversed cylinders or reversed spherical shape for $P>1$.

3. Structure of microemulsions

The micro-structure of microemulsions has been elucidated by various techniques developed recently, which include a static or dynamic light scattering, a dielectric relaxation, a time-resolved fluorescence or phosphorescence quenching, an electric field or temperature jump, a small-angle neutron scattering (SANS) and a small-angle X-ray scattering (SAXS) [14]. These techniques can afford fruitful information about the core and surface monolayer structure, the particle size distribution, the polydispersity, the droplet clustering and diffusion dynamics, the interdroplet exchange rate and the monolayer fluidity. The rather classical methods of the measurements of viscosity, interfacial tension and conductivity are still very reliable and informative.

The most versatile method for the determination of the size of the microemulsion droplets is SANS by using contrast variation method [15]. The spontaneous radii R_0 of AOT microemulsion was determined by SANS and the least effect of the counter cation radii on the R_0 was concluded [16]. The extent of alkane penetration into the surfactant monolayer in w/o microemulsion was studied by SANS and a significant mixing was found for phosphatidylcholine and *n*-octadecyl-*n*-dodecyldimethylammonium bromide monolayers [17]. The SAXS measurement also can afford reliable data on the radius of water core of w/o microemulsion droplets. The AOT microemulsion radius determined by SAXS in the Winsor II region can be related to the water-to-AOT mole-ratio w in the microemulsion phase,

$$R_0/\mathrm{nm} = 0.16w + 1.2$$

where $0.16w$ is equivalent to the radius of the waterpool [18].

The polydispersity and size distribution of microemulsion are also important parameters for physical description of microemulsions. Thermodynamic evaluation predicted a size polydispersity of 0.1–0.2 for Winsor II microemulsions, where the width of the size distribution was determined by the interfacial tension of the planar oil–water interface [19].

The curvature of the monolayer of a microemulsion droplet was shown to determine the type and the stability of the microstructure [20]. The study of the time-resolved fluorescence and dynamic light scattering on the o/w microemulsions stabilized by a range of alkylpoly(oxyethylene glycol ether) revealed that the tail group areas of the surfactants increase with increasing droplet size [21]. The relative radius polydispersities were in the range 0.1–0.2 and decreased with increasing overall surfactant chain-length.

Dynamic properties of microemulsion droplets are very important in understanding the conductivity, chemical reactions and mass transfer in microemulsions. Phosphorescence quenching study of Tb^{3+} complex ion in w/o microemulsions demonstrated the exchange of quencher between clusters of microemulsions which took place in ms time range [22]. On the other hand, the exchange of the fluorescence probe molecules between the droplets occurred in μs time range. This exchange was thought to correspond to the time required for the droplet coalescence and reseparation [23]. Laser T-jump experiment succeeded in measuring the relaxation time of AOT w/o microemulsions on a few μs scale and determined the bending elastic modulus of the AOT interfacial monolayer as 0.4 kT at large water content [24]. Laser E-jump study also could measure the transient electric birefringence which is a consequence of the creation of induced micellar dipoles and the reequilibration process in 100 μs range [25]. These fast exchange dynamics are very favorable for the use of microemulsions in chromatographic separation systems.

4. Microscopic partition and reaction in microemulsions

Characteristic solvent effects of microemulsions, as reported in the stability of acids and bases and the reactivity of metal ions, are beneficial to various separation methods using microemulsions as media. Microemulsions contain finely divided domains of oil and water topologically ordered by surfactant at the internal interfaces. Therefore, a solute can distribute among the microscopic water phase, oil phase and interface. This microscopic partitioning greatly affects the solubility and reactivity. Solubilization of acidic and basic azo dyes in the microemulsions composed of SDS–1-butanol–toluene–water or dodecyltrimethylammonium bromide (DTAB)–1-butanol–toluene–water was much enhanced over that in pure solvents [26]. The more surfactant-like the dye becomes, the greater the solubility in water-rich microemulsions. The primary site for the dye solubilization is thought the surfactant-rich interfacial region separating oil-rich and water-rich domains. The keto–enol tautomerization and dissociation equilibria of β-diketones in o/w microemulsions were highly dependent on the charge types of the surfactant and the volume fraction of the organic component [27]. The enol fraction in the microemulsions increased with an increase of the volume fraction, indicating the higher stability of the enol form in the organic solvent.

The apparent dissociation constants in cationic cetyltrimethylammonium bromide (CTAB) microemulsions were larger than those in the anionic SDS and non-ionic Triton X-100 microemulsions even in an aqueous solution, by the electrostatic stabilization of enolate ion at the interface of the oil droplets (Table 1).

The organic droplets in o/w microemulsions can be thought analogous to an organic phase in solvent extraction. Synergistic extraction of lanthanide(III) ions with β-diketone and trioctylphosphine oxide (TOPO) has been established in bulk two-phase systems [28]. Analogous behavior was observed in SDS o/w microemulsions. The formation of the adduct complexes of Eu(III) and Sm(III) with thenoyltrifluoroacetone or 2-naphthoyltrifluoroacetone and TOPO in the oil droplets was concluded from an enhancement of the fluorescence intensity characteristic for these fluorescent adducts (Fig. 3) [29]. The composition of the adduct was confirmed as metal–β-diketone–TOPO = 1:3:2 which was consistent with those observed in bulk two-phase system. The adduct formation constants determined in the o/w microemulsion systems are listed in Table 2, in which the magnitude of the constants is less than those obtained in inert organic solvents, because of

Table 1
Apparent dissociation constants and adsorption parameters of β-diketones at 25°C [27]

Solvent	φ[a]	Benzoylacetone		Benzoyltrifluoroacetone		Naphtoyltrfluoroacetone	
		pK_a (app)	$K'_L\varphi_i$[b]	pK_a (app)	$K'_L\varphi_i$	pK_a (app)	$K'_L\varphi_i$
0.01 *M* SDS	0.023	9.98	–	6.88	1.9	7.33	18
SDS–ME[c]	0.120	9.93	0.04	6.60	8.6	6.89	50
SDS–ME[d]	0.389	10.29	0.44	6.84	10	6.89	$1.3\cdot10^2$
TX100–ME[e]	0.107	9.73	0.52	6.11	63	–	
CTAB–ME[f]	0.127	8.27	44	4.38	$2.8\cdot10^3$	–	
pK_a in aq.		8.70[g]		6.31[i]		6.27[i]	

[a] Volume fraction of organic components.
[b] $K'_L=(L^-)_i/(L^-)$ and φ_i is the volume fraction of interphase.
[c] Water–SDS–1-butanol–heptane (89.30:3.31:6.61:0.80, v/v).
[d] Water–SDS–1-butanol–heptane (65.14:9.30:18.59:6.97, v/v).
[e] Water–Triton X-100–octane (89.30:9.92:0.80, v/v).
[f] Water–CTAB–1-butanol–octane (89.30:3.31:6.61:0.80, v/v).
[g] [57].
[i] [58]

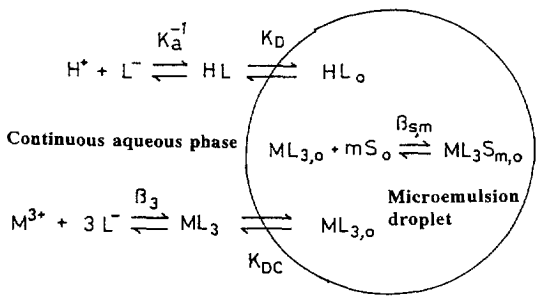

Fig. 3. Schematic illustration of the adduct formation equilibria of tris(β-diketonato)lanthanide(III), $ML_{3,o}$, with TOPO, S_o, in o/w microemulsion droplet. K_a, K_D, β_3, K_{DC} and $\beta_{s,m}$ refer to the dissociation constant of β-diketone, the distribution constant of β-diketone, the formation constant of ML_3, the distribution constant of ML_3 and the adduct formation constant, respectively.

the solvating effect of 1-butanol to the ligands and the metal ions.

The chemical kinetics are largely affected by the characteristic properties of the media which are used. The reaction rate of $Fe(phen)_3^{2+}$ complexes with hydroxide ion was investigated in 2-butoxyethanol–decane–water microemulsions and the marked acceleration in the reaction was interpreted by an adsorption of the complex ion at the interface of microdroplets [30]. Catalytic reduction of *trans*-1,2-dibromocyclohexane with electrochemically generated Co(I) complexes was faster in a bicontinuous microemulsion than in a w/o microemulsion, which was caused by a larger interfacial area of the bicontinuous system [31].

The complexations of metal ion in microemulsions is gaining a continuing interest in relation to the locale of the metal–extractant reaction. From NMR and UV–Vis spectrometry for the reaction of Ni^{2+} with an alkylated derivative of 8-hydroxyquinoline, the reaction is thought to be taking place at the microscopic interface [32].

Table 2
Adduct formation constants in o/w microemulsion droplets at 25°C[a] [29]

β-diketone	pK_a	log $\beta_{s,2}$	
		Eu(III)	Sm(III)
Thenoyltrifluoroacetone	6.17[b]	7.23±0.53	6.37±1.04
Naphtoyltrifluoroacetone	6.27[c]	6.13±0.62	6.03±0.36

[a] Water–SDS–1-butanol–heptane (89.30:3.31:6.61:0.80, v/v).
[b] [59].
[c] [58].

5. Microemulsions in solvent extraction

5.1. Microemulsion extraction of metal complexes

The extraction of metal ions in aqueous phase with w/o microemulsion organic phase (Winsor II system) is often very effective for the acceleration of extraction as well as for the improvement of extractability [33]. The increase of the extraction rate was explained by an enormous rise of the micro-interfacial surface area in the w/o microemulsion phase and the participation of the microemulsion globes to transport metal ions from the aqueous phase to the organic phase. Thus, the reaction can occur both on the macroscopic and microscopic interfaces. A direct forward or reverse transfer of the metal ions inside the microdroplet in the organic phase is also possible by a coalescence with the interfacial surfactant film.

The extraction rate of Ga(III) from aqueous sodium hydroxide and Al(III) solutions with 7-(1-ethenyl-3,3,5,5-tetramethylhexyl)-8-quinolinol in kerosene was increased by addition of an alcohol together with the sodium salt of a long chain carboxylic acid. The organic phase of this system was a w/o microemulsion. The radius of the microemulsion droplets has been estimated to be 2.0–5.0 nm [34].

The reaction mechanism of complexation in w/o microemulsion systems was studied to get an insight into the role of the interface in solvent extraction systems. The kinetics of complexation of Ni^{2+} with either 8-hydroxyquinoline (HQ) or 7-(4-ethyl-1-methyloctyl)-8-hydroxyquinoline (C_{11}-HQ, an active component of Kelex 100) were studied by a stopped-flow technique in SDS–1-pentanol–dodecane–water microemulsions [35,36]. The reaction appeared to be essentially a 'bulk reaction' with HQ and an 'interfacial reaction' with Kelex 100. ^1H NMR chemical shift, linewidth and relaxation time measurements revealed that C_{11}-HQ was essentially located in the amphiphilic palisade of o/w microemulsion which

was prepared from CTAB–butanol–water, when the surfactant to extractant ratio becomes higher than 8 [37].

The complexation of metal ions by the solubilized extractant was used for the development of a new extraction process. An ultrafiltration method succeeded in the selective recovery of the different metal ions from their complex with HQ or C_{11}-HQ in the microdroplets as shown in Fig. 4 [38].

The water uptake in w/o microemulsion phase in Winsor II system was greatly affected by the presence of extractants and metal ion. The water content in AOT–isooctane phase was substantially increased by the addition of di(2-ethylhexyl)dithiophosphoric acid and Cu^{2+} [39].

5.2. Microemulsion extraction of biological compounds

It has been shown that different protein molecules exhibit different affinities for w/o microemulsion phase, which can be used to achieve a selective separation of a protein of interest from other material found in an aqueous phase broth [40]. The protein partitioning phenomena were understood through the use of thermodynamic model [41], while the transfer kinetic phenomena have begun to be examined very recently. The interfacial mass transfer coefficients for the forward transfer of proteins α-chymotrypsin and cytochrome *c* showed strong dependence on pH and salt concentration [42]. This indicated that the electrostatic interaction between a protein particle and the bulk interface has the dominant role in the mass transfer rates. Back transfer rates were slower than those for forward transfer, because of the slow coalescence rate of the protein-filled micelle with the bulk interface. In some cases, the protein itself also participates in the kinetic mechanism of the mass transfer. In the mass transfer of tryptophan between an aqueous phase and a w/o microemulsion (isooctane–AOT–water), the tryptophan fraction in the shell of the bud determined the residence time of the buds at the interface and therefore the degree of equilibration [43]. The extraction rate of α-chymotrypsinogen A (CTN) by the w/o microemulsion in a stirred cell apparatus was found to be composed of two processes: a fast extraction and an ~100-times slower subsequent back-extraction. The adsorption of AOT onto the surface of CTN through the electrostatic interaction converts CTN from a hydrophilic to hydrophobic state. This is responsible for the fast extraction process. The adsorption of AOT by a hydrophobic interaction with CTN in turn makes the CTN-surface hydrophilic, which is attributed to the slow-back extraction (Fig. 5) [44].

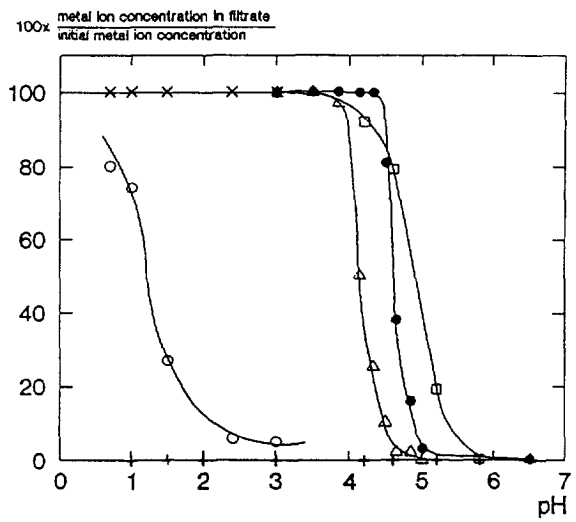

Fig. 4. Ultrafiltration experiments: percent of metal ion concentration found in the filtrate reported to the initial concentration vs. pH after acid dissociation in the CTAB–1-butanol micellar solution. Analytical extractant and metal ion concentrations: $3.4 \cdot 10^{-3}$ *M* and $1.7 \cdot 10^{-4}$ *M*, respectively. HQ with Ni^{2+}–Co^{2+}: (△) Ni^{2+}; (●) Co^{2+}. C_{11}-HQ with Ni^{2+}–Cu^{2+}: (×) Ni^{2+}; (○) Cu^{2+}. C_{11}-HQ with Ni^{2+}–Ci^{2+}: (□) Ni^{2+}; (+) Co^{2+} [38].

6. Microemulsions in HPLC

The properties of the eluent are essential factors governing the efficiency in HPLC. Micellar solutions were used as an eluent of a reversed-phase LC for the first time by Armstrong and Henry, but the efficiency was not improved by the addition of surfactants [45]. The w/o microemulsions composed of water–AOT–hexane was introduced for a normal phase LC by Hernandez et al. [46]. Systematic research using water–AOT–heptane as mobile phase in an unbonded silica column was carried out recently [47]. The capacity factor depended drastically upon the physicochemical structure described by using the water–AOT molar ratio, *w*. When $w < 10$,

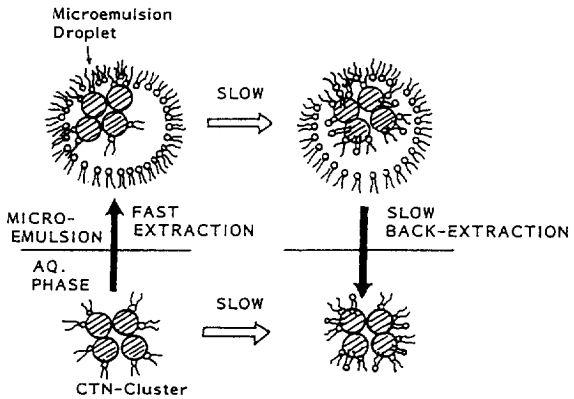

Fig. 5. Illustrative diagram showing CTN extraction mechanism. The fast extraction proceeds by the adsorption of AOT molecules on the surface of CTN, which converts hydrophilic CTN to a hydrophobic state. The slow back-extraction occurs by the additional adsorption of AOT, which in turn converts hydrophobic CTN to hydrophilic state [44].

the column dead-volume was decreased up to 50% with increase of the water content because of the AOT adsorption on the silica stationary phase. The o/w microemulsion composed of heptane–SDS–pentanol–water was also examined as a mobile phase in reversed-phase HPLC for the separation of benzene derivatives [48]. A higher content of the active blend SDS–pentanol produced a higher efficiency for the alkylbenzene peaks.

7. Microemulsions in CE

Capillary electrophoresis (CE) is one of the most attractive techniques in analytical separation which has been developed over the last decade. CE has extensively been utilized not only as a microseparation technique but also as a powerful tool for determining some physicochemical properties such as dissociation constants and diffusion coefficients, because of its high efficiency, good reproducibility, automatization suitability, rapid analysis time and micro scale sample amount. In particular, micellar electrokinetic chromatography (MEKC) is an excellent tool for the analyses of neutral compounds. The separation principle of MEKC is based on the partitioning of the solute between an aqueous phase and a micellar phase [49,50]. MEKC has been applied for various types of analytes including drugs, peptides, nucleic acid constituents and so on. However, a poor solubilization capacity of micelles for hydrophilic molecules and large molecules limited the application of MEKC in some cases. Also, the separation window in MEKC, which is the range in the migration time used for the separation, is almost fixed and not controllable. The possibility of utilizing microemulsions in electrokinetic chromatography of ionic and non-ionic samples has been demonstrated for the first time by Watarai [51]. The o/w microemulsions are similar to micelles in that they can solubilize hydrophobic compounds, but with a much larger capacity because of the larger droplet size. The higher capacity for solubilization can permit the incorporation of a variety of hydrophobic additives as well as a wide variety of samples. Introduction of o/w microemulsions as the separation media significantly improved the solubilization capacity and the separation window.

The microemulsion composed of water–SDS–1-butanol–heptane (89.28:3.31:6.61:0.80, v/v) was used as the media for the separation of naphthalene derivatives, ketones and β-diketones [51,52]. The direction of migration of the o/w microemulsion droplets is determined by the relative magnitude of the electrophoretic velocity of the negatively charged droplets and the bulk flow to the negative end of the capillary caused by an electroosmosis which depends on pH, the nature of buffering compound and its concentration, and other factors affecting the zeta potential of the capillary wall. Under pH 7.33 and 0.05 *M* acetate buffer, the electrophoretic migration of the negatively charged droplets was faster than the electroosmotic flow and then a more hydrophobic solute which can be incorporated into the droplets migrated faster as shown in Fig. 6. On the other hand, in alkaline conditions, the electroosmotic flow was superior to the electrophoresis of the droplets and the more hydrophilic solute was detected at shorter time as shown in Fig. 7. The increase in the organic components from 0.12–0.35 in the volume fraction resulted in poor resolution (Fig. 8). This means that the usable o/w microemulsion region is restricted within L_1 region except a bicontinuous or percolation region. Water in oil microemulsion region is difficult to use without some modification. The correlation between the degree of solubilization

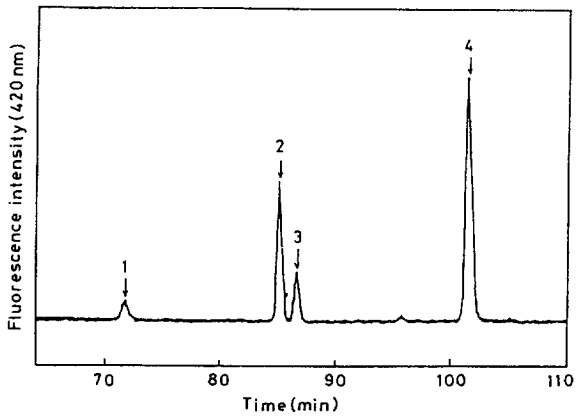

Fig. 6. Electropherogram of (1) anthracene, (2) α-naphthol, (3) β-naphthol and (4) α-naphtylamine, pH 7.33 by 0.05 *M* acetate in water –SDS–1-butanol–heptane (89.28:3.31:6.61:0.80, v/v), 18 μA and 10 kV [52].

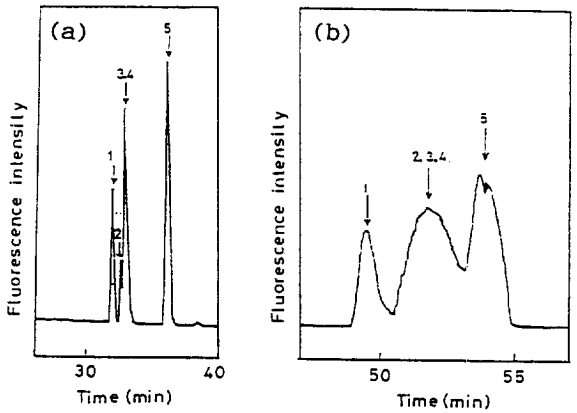

Fig. 8. Electropherograms of (1) anthracene, (2) anthrone, (3) α-naphthol, (4) β-naphthol and (5) α-naphthylamine; Volume fractions of the SDS microemulsions are (a) 0.120 and (b) 0.349 [52].

of naphthalene derivatives and the capacity factors was demonstrated as listed in Table 3. The degree of solubilization was determined by a fluorescence quenching method using Co(II) ion or Ni(II) ion as selected quenchers. The results listed in the table indicate that the more solubilized solute can migrate faster. The migration order of solutes could be reversed by changing the pH which varied the charge

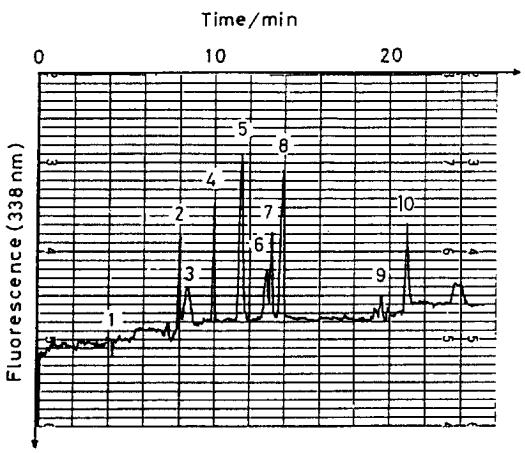

Fig. 7. Separation of ketones and β-diketones detected by the indirect fluorescence method; Excitation at 279 nm, 10 kV, 40 μA, 5 s sampling time, pH 9.5; 1 = solvent peak, 2 = 2-acetylthiophene, 3 = acetylacetone, 4 = acetophenone, 5 = benzoylacetone, 6 = pivaloyltrifluoroacetone, 7 = thenoyltrifluoroacetone, 8 = benzoyltrifluoroacetone, 9 = 2-naphthoyltrifluoroacetone, 10 = system peak. Microemulsion is the same as Fig. 6 [51].

of solute as well as the magnitude of zeta potential. Table 4 shows the capacity factors of acetylacetone and benzoylacetone, which were reversed by the change of pH, reflecting the change in the degree of dissociation. Also, the extension of the migration-time window in the SDS microemulsions over the SDS micelle system is shown in this table. This is owing to the larger electrophoretic mobility of the SDS microemulsion over that of the SDS micelles [53]. Although similar observations have been reported in other systems [54], further research is required to explain the higher migration velocity of SDS microemulsion from the molecular point of view.

Recently, the microemulsion electrokinetic chromatography was applied for the evaluation of the hydrophobicity of various kinds of organic compounds. The logarithm of the capacity factors was highly correlated with the log *P* values and further showed slightly better correlation to the toxicity data of phenol derivatives. Thus, it was proposed as a biologically useful alternative hydrophobic parameter [54].

Although an analytical application of the microemulsion CE is still limited, an interesting result is obtained in an analysis of pesticides, which is difficult by MEKC or GLC, by the o/w microemulsion CE using SDS–water–1-butanol–heptane (Fig. 9) [55]. ^{31}P NMR shift of organophosphorus pes-

Table 3
The solubilization indices $I_F/(I_{F0}-I_F)$, the capacity factors k' and the partition coefficients log P of naphthalene derivatives[a] [52]

Solute	$I_F/(I_{F0}-I_F)$[b]	k' (pH 3.0)[c]	k' (pH 7.3)[c]	log P[d]
Naphthalene	4.18	0		3.45
α-Naphthol	2.74	0.065	0.187	2.84
Anthracene	1.98		0	4.77
β-Naphthol	1.80	0.065	0.210	2.84
N-Acetyl-α-naphthylamine	1.44	0.249		1.67
1,4-Naphthoquinone	1.10	0.463		2.11
Sodium 2-naphthol-6-sulfonate	0.16	0.453		–
α-Naphthylamine	0.13		0.419	2.22

[a] Water–SDS–1-butanol–heptane (89.3:3.31:6.61:0.80, v/v).
[b] I_{F0} and I_F refer to the fluorescence intensities of the solute in microemulsions (pH 5.9–6.4) containing 0.09 *M* Zn(II) and 0.09 *M* Co(II), respectively.
[c] $k'=(t_R-t_0)/t_0$ where t_0 is the migration time of naphthalene or anthracene and t_R is that of the other solutes.
[d] The values of log P (1-octanol–water) for the neutral compounds were estimated from [60].

ticides in the microemulsion correlated with the migration order of the solutes, indicating the microenvironment of the locale of the solute molecule in the heterogeneous system. The separation of nucleic acid constituents is one of the important subjects which have been extensively studied in the field of bioanalytical chemistry. Migration characteristics of bases and nucleosides in CE using o/w microemulsions composed of SDS–heptane or toluene–water–1-butanol have recently been attempted [56]. The differences between log k' values of the bases and the corresponding nucleosides were almost constant independent of the nature of nucleosides. This meant that the sugar in nucleosides gave a constant contribution to the log k' values.

Until now, only o/w microemulsions have been studied as separation media in CE by an analogous manner with normal micelles, because of the intrinsic poor conductivity in w/o microemulsions. However, a migration of water droplets in AOT microemulsion could be attained by the addition of an appropriate electrolyte which enhanced the conductivity (H. Watarai and T. Sugiyama, unpublished results).

Since some novel results have been reported as reviewed here, further attempts to use various types of microemulsions as separation media are now required for the development of the microemulsion

Table 4
Migration parameters of acetylacetone (AA) and benzoylacetone (BA) [52]

Solvent	pH	t_{ME}/t_0	k' (AA)[a]	k' (BA)[a]
SDS (0.1 *M*)	9.0	3.6	0.56	6.70
	11.0	3.8	2.89	1.85
SDS–ME[b]	9.0	5.5	0.89	4.57
	11.0	8.4	4.01	2.99

[a] Water–SDS–1-butanol–heptane (89.3:3.31:6.61:0.80, v/v).
[b] Capacity factors were calculated by $k'=(t_{ME}/t_0)(t_R-t_0)/(t_{ME}-t_R)$.

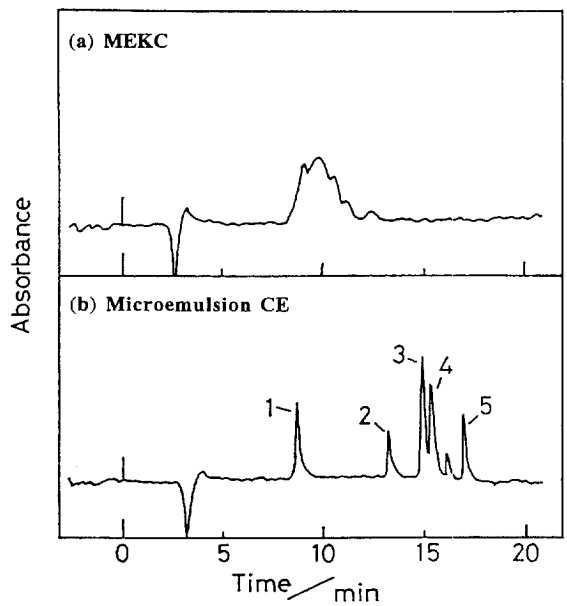

Fig. 9. Comparison of the electropherograms of pesticides; (a) MEKC in 3.6% SDS solution and (b) o/w microemulsion CE which composition is the same with that in Fig. 6; (1) Formothion, (2) Malathion, (3) MEP, (4) IBP and (5) Ethion; 10 kV, 25 μA, 222 nm, pH 9.5 [55].

CE, both in fundamental researches and in practical applications.

References

[1] E.W. Kaler, S. Prager, J. Colloid Interface Sci. 86 (1982) 359.
[2] P.A. Winsor, Trans. Faraday Soc. 44 (1948) 376.
[3] J. Van Nieuwkoop, G. Snoei, J. Colloid Interface Sci. 103 (1985) 417.
[4] J. Van Nieuwkoop, G. Snoei, J. Colloid Interface Sci. 103 (1985) 400.
[5] E. Paatero, J. Sjoblom, Hydrometallurgy 25 (1990) 231.
[6] K. Shinoda, Prog. Colloid Polym. Sci. 68 (1983) 1.
[7] K. Ogino, M. Nakamae, M. Abe, J. Phys. Chem. 93 (1989) 3704.
[8] A. Shioi, M. Harada, K. Matsumoto, J. Phys. Chem. 95 (1991) 7495.
[9] D.C. Steytler, D. Lee Sargeant, G.E. Welsh, B.H. Robinson, R.K. Heenan, Langmuir 12 (1996) 5312.
[10] K.D. Tapas, Adv. Colloid Interface Sci. 59 (1995) 95.
[11] M. Goto, T. Ono, F. Nakashio, T.A. Hatton, Biotech. Techn. 10 (1996) 141.
[12] J.N. Israelachvili, D.J. Mitchell, B.W. Ninham, J. Chem. Soc., Faraday Trans. II 72 (1976) 1525.
[13] D.J. Mitchell, B.W. Ninham, J. Chem. Soc., Faraday Trans. II 77 (1981) 601.
[14] A. Shioi, M. Harada, M. Tanabe, Langmuir 12 (1996) 3201.
[15] R. Strey, J. Winkler, L. Magid, J. Phys. Chem. 95 (1991) 7502.
[16] J. Eastoe, S. Chatfield, R. Heenan, Langmuir 10 (1994) 1650.
[17] J. Eastoe, K.J. Hetherington, D. Sharpe, J. Dong, R.K. Heenan, D. Steytler, Langmuir 10 (1994) 2547.
[18] M. Harada, M. Adachi, A. Shioi, K. Kurumada, K. Kawakami, Int. J. Soc. Mat. Eng. for Resources 4 (1996) 2.
[19] J.C. Eriksson, S. Ljunggren, Langmuir 11 (1995) 1145.
[20] D.F. Evans, D.J. Mitchell, B.W. Ninham, J. Phys. Chem. 90 (1986) 2817.
[21] P.D.I. Fletcher, R. Johansson, J. Chem. Soc. Faraday Trans. 90 (1994) 3567.
[22] H. Mays, J. Pochert, G. Ilgenfritz, Langmuir 11 (1995) 4347.
[23] S. Clark, P.D.I. Fletcher, X. Ye, Langmuir 6 (1990) 1301.
[24] C. Petit, J.F. Holzwarth, M.P. Pileni, Langmuir 11 (1995) 2405.
[25] H.M. Chen, Z.A. Schelly, Langmuir 11 (1995) 758.
[26] K.R. Wormuth, L.A. Cadwell, E.W. Kaler, Langmuir 6 (1990) 1035.
[27] H. Watarai, M. Takano, N. Suzuki, Bull. Chem. Soc. Jpn. 65 (1992) 170.
[28] S. Nakamura, Y. Surakitbanharn, K. Akiba, Anal. Sci 6 (1990) 295.
[29] H. Watarai, K. Ogawa, N. Suzuki, Anal. Chim. Acta 277 (1993) 73.
[30] M.J. Blandmer, J. Burgess, B. Clark, P.P. Duce, J. Chem. Soc., Faraday Trans. 80 (1984) 739.
[31] De-L. Zhou, J. Gao, J.F. Rusling, J. Am. Chem. Soc. 117 (1995) 1127.
[32] C. Tondre, D. Canet, J. Phys. Chem. 65 (1991) 4810.
[33] J. Szymanowski, C. Tondre, Solv. Extr. Ion Exch. 12 (1994) 873.
[34] F. Fourre, D. Bauer, J. Lemerie, Anal. Chem. 55 (1983) 662.
[35] C. Tondre, M. Boumezioud, J. Phys. Chem. 93 (1989) 846.
[36] M. Boumezioud, H.S. Kim, C. Tondre, Colloids Surfaces 41 (1989) 255.
[37] W. Richmond, P. Rubini, C. Tondre, Solv. Extr. Ion Exch. 13 (1995) 541.
[38] M. Ismael, C. Tondre, Sep. Sci. Technol. 29 (1994) 651.
[39] E. Paatero, J. Sjoblom, S.K. Datta, J. Colloid Interface Sci. 138 (1990) 388.
[40] T.A. Hatton, in: J.F. Scamehorn, J.H. Harwell, (Eds.) Surfactant-Based Separation Processes, Dekker, New York, 1989, p. 55–90.
[41] R.S. Rahaman, T.A. Hatton, J. Phys. Chem. 95 (1991) 1799.
[42] S.R. Dungan, T. Bausch, T.A. Hatton, P. Plucinski, W. Nitsch, I. Colloid Interface Sci. 145 (1991) 33.
[43] P. Plucinski, W. Nitsch, Langmuir 11 (1995) 4691.
[44] K. Kawakami, M. Harada, M. Adachi, A. Shioi, Colloids Surfaces 109 (1996) 217.
[45] D.W. Armstrong, S.J. Henry, J. Liq. Chromatogr. 3 (1980) 657.
[46] M.A. Hernandez-Torres, J.S. Landy, J.G. Dorsey, Anal. Chem. 58 (1986) 744.
[47] A. Berthod, O. Nicolas, M. Porthault, Anal. Chem. 62 (1990) 1402.
[48] A. Berthod, M. De Carvalho, Anal. Chem. 64 (1992) 2267.
[49] S. Terabe, K. Otsuka, K. Ichikawa, A. Tuchiya, T. Ando, Anal. Chem. 56 (1984) 111.
[50] S. Terabe, K. Otsuka, T. Ando, Anal. Chem. 57 (1985) 834.
[51] H. Watarai, Chem. Lett., (1991) 391.
[52] H. Watarai, K. Ogawa, M. Abe, T. Monta, I. Takahashi, Anal. Sci. 7(Suppl.) (1991) 245.
[53] S. Terabe, N. Matsubara, Y. Ishihama, Y. Okada, J. Chromatogr. 608 (1992) 23.
[54] Y. Ishihama, Y. Oda, K. Uchikawa, N. Asakawa, Anal. Chem. 67 (1995) 1588.
[55] T. Fukumoto, H. Watarai, Bunsekikagaku 46 (1997) 439.
[56] H. Watarai, M. Sekiguchi and T. Sugiyama, to be submitted.
[57] G.V. Hartland, F. Grieser, L.R. White, J. Chem. Soc. Faraday Trans. 1(83) (1987) 591.
[58] H. Watarai, K. Kamade, S. Yokoyama, Solv. Extr. Ion Exch. 7 (1989) 361.
[59] E.M. Larsen, G. Terry, J. Am. Chem. Soc. 75 (1953) 1560.
[60] A. Leo, C. Hansch, D. Elkins, Chem. Rev. 71 (1971) 525.